

The glaciers of the Hindu Kush Himalayas: current status and observed changes from the 1980s to 2010

Samjwal Ratna Bajracharya, Sudan Bikash Maharjan, Finu Shrestha, Wanqin Guo, Shiyin Liu, Walter Immerzeel & Basanta Shrestha

To cite this article: Samjwal Ratna Bajracharya, Sudan Bikash Maharjan, Finu Shrestha, Wanqin Guo, Shiyin Liu, Walter Immerzeel & Basanta Shrestha (2015) The glaciers of the Hindu Kush Himalayas: current status and observed changes from the 1980s to 2010, International Journal of Water Resources Development, 31:2, 161-173, DOI: [10.1080/07900627.2015.1005731](https://doi.org/10.1080/07900627.2015.1005731)

To link to this article: <https://doi.org/10.1080/07900627.2015.1005731>



© 2015 The Author(s). Published by Taylor & Francis.



Published online: 03 Feb 2015.



Submit your article to this journal [↗](#)



Article views: 6794



View related articles [↗](#)



View Crossmark data [↗](#)



Citing articles: 54 View citing articles [↗](#)

The glaciers of the Hindu Kush Himalayas: current status and observed changes from the 1980s to 2010

Samjwal Ratna Bajracharya^{a*}, Sudan Bikash Maharjan^a, Finu Shrestha^a, Wanqin Guo^b, Shiyin Liu^b, Walter Immerzeel^c and Basanta Shrestha^a

^aInternational Centre for Integrated Mountain Development, Kathmandu, Nepal; ^bCold and Arid Regions Environmental and Engineering Research Institute, Chinese Academy of Sciences, Lanzhou, China; ^cDepartment of Physical Geography, Utrecht University, the Netherlands

(Received 25 August 2014; accepted 6 January 2015)

The fate of the Hindu Kush Himalayan glaciers has been a topic of heated debate due to their rapid melting and retreat. The underlying reason for the debate is the lack of systematic large-scale observations of the extent of glaciers in the region owing to the high altitude, remoteness of the terrain, and extreme climatic conditions. Here we present a remote sensing-based comprehensive assessment of the current status and observed changes in the glacier extent of the Hindu Kush Himalayas. It reveals highly heterogeneous, yet undeniable impacts of climate change.

Keywords: Landsat; remote sensing; glacier area changes; decadal

Introduction

The Hindu Kush Himalayan (HKH) region is the freshwater tower of South Asia. It has the highest concentration of snow and glaciers outside the polar region, and thus has been called the Third Pole (Dyhrenfurth, 1955). The snow and glacier meltwater plays a pivotal role in the water supply for those river basins that are arid downstream, in particular where there are large irrigation systems that depend on upstream water resources. Mountain ranges are particularly sensitive to climate change, and the HKH region is no exception. Changes in the glaciers may have a significant impact on the quantity and timing of water availability (Rabatel et al., 2013). A comprehensive understanding of the extent and nature of changes in glaciers will support downstream hydrological planning and water resource management (Rankl, Kienholz, & Braun, 2014). We focus on the development of the glacier area over decades, to understand future change and offer a possible evaluation of future water quantity and availability.

There is a large variation in glacier response in the region owing to the diverse terrain and climates. There are transitions from colder to drier and a wetter (monsoon dominated) to warmer climate from west to east and from north to south. Overall, the glaciers in the region are retreating or shrinking and thinning due to climate change (Fujita & Nuimura, 2011; Kargel, Cogley, Leonard, Haritashya, & Byers, 2011; Kaser, Cogley, Dyurgerov, Meier, & Ohmura, 2006; Scherler, Bookhagen, & Strecker, 2011; Zemp, Hoelzle, & Haeberli, 2009). Some studies report a different behaviour of glaciers in the Karakoram (Hewitt, 2005, 2011; Scherler et al., 2011), which may be explained by a positive trend in winter precipitation and limited warming during the melt season (Archer & Fowler, 2004; Tahir, Chevallier, Arnaud, & Ahmad, 2011). Climate change also leads to the expansion

*Corresponding author. Email: sabajracharya@icimod.org

and formation of glacial lakes, which could lead to an increase in glacial lake outburst floods. A number of such floods have already been reported in the region (Bajracharya & Mool, 2010; Bajracharya, Mool, & Shrestha, 2007; Richardson & Reynolds, 2000).

Despite the importance of the HKH region, there is a lack of consistent and homogeneous glacier data. Most studies focus on small areas and present a regional overview. Several interlinked global glacier inventory initiatives exist, such as the World Glacier Monitoring Service (Haerberli, Böschi, Sherler, Østrem, & Wallèn, 1989), Global Land and Ice Measurements from Space (GLIMS) (Raup et al., 2007), the GlobGlacier project (Paul et al., 2010), and the Randolph Glacier Inventory (Pfeffer et al., 2014). However, none of these initiatives has resulted in a consistent and complete glacier inventory for the HKH region. Such a regional glacier database, based on a standardized method, is therefore urgently needed as a benchmark against which changes can be assessed. Recently, an inventory of glaciers, including debris-covered (DC) glaciers, has been developed for the entire HKH region using remote-sensing data (Bajracharya & Shrestha, 2011; Bolch et al., 2012). The glacier outlines were compiled using a semi-automated remote-sensing method with topographic information obtained from the void-filled version of the Shuttle Radar Topography Mission digital elevation model (SRTM DEM). The comprehensive assessment of glaciers is based on the status as of 2005 \pm 3 years, whereas the extent of glacier change is based on a temporal series of Landsat images since the 1980s.

Study area

The HKH region extends from 15.95° to 39.31° N latitude and 60.85° to 105.04° E longitude, encompassing an area of about 4.2 million km² and extending across all or part of the eight countries of Afghanistan, Bangladesh, Bhutan, China, India, Myanmar, Nepal and Pakistan (Bajracharya & Shrestha, 2011). There are high concentrations of snow and glaciers in the mountains of the region. Meltwater from snow and glaciers feeds the 10 largest river systems in Asia: the Amu Darya, Indus, Ganges, Brahmaputra, Irrawaddy, Salween, Mekong, Yangtze, Yellow and Tarim (Immerzeel, Van Beek, & Bierkens, 2010; Kaser, Großhauser, & Marzeion, 2010).

Four representative basins were selected for decadal glacier change analysis: the Wakhan Corridor in Afghanistan, the Shyok Basin in Pakistan, the Imja Valley in Nepal, and the Lunana region in Bhutan (Figure 2).

Data and methods

Data

This study used more than 200 orthorectified Landsat 7 ETM + L1G scenes from the Global Land Cover Facility (<http://www.landcover.org>) from 2005 \pm 3 years. Images with a minimum of cloud and snow cover were selected. The Landsat 7 ETM + images suffer from a scan-line corrector failure, causing a wedged-shaped scan-to-scan gap. Prior to analysis, the scan-line gaps were filled using a specifically developed software extension in the ENVI image-processing package. We used a 90 m resolution SRTM DEM to derive the attribute data for each glacier.

For the decadal glacier change analysis, Landsat 5 MSS, Landsat 7, and Landsat 7 ETM + images were used. To delineate the glacier outline, the images should have low snow and be cloud-free; however, the freely downloadable images rarely meet the ideal requirements, hence images must be selected from a range of years rather than a single

year. Landsat 5 MSS images from 1976 to 1979 were used to approximate 1980 (hereafter referred to as ~1980); Landsat 7 TM images from 1988 to 1992, for 1990; Landsat 7 ETM + from 1999 to 2001, for 2000; and Landsat 7 ETM + from 2009 to 2011, for 2010. In each case, the images with the least snow cover and no cloud cover were selected.

Glacier outline for 2005

Most glaciers are clearly visible as a clean-ice (CI) surface, but some have debris cover (DC) at their tongues. The spectral uniqueness of CI glaciers in the visible and near-infrared bands of the electromagnetic spectrum allows the use of simple algorithms. However, the delineation of DC glaciers poses challenges because of the non-unique spectral signatures and illumination errors due to effects from surrounding materials.

The images were first segmented using object-based image classification in eCognition software (Figure 1) with different parameter settings (type of variable and threshold value) for CI and DC glaciers (Bajracharya, Maharjan, & Shrestha, 2014). The Normalized

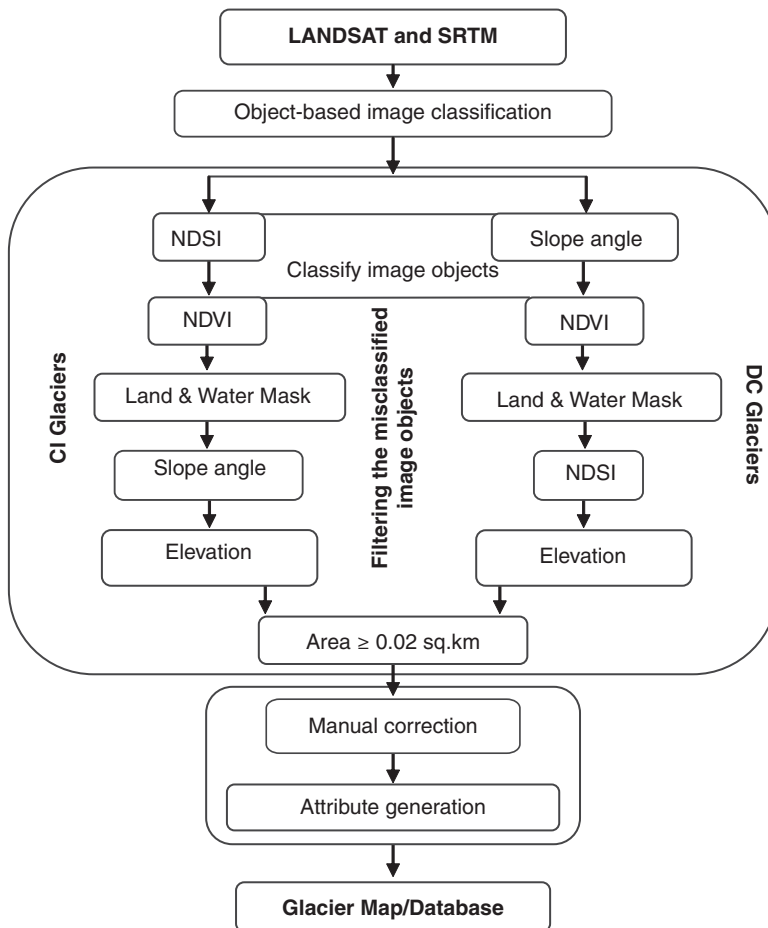


Figure 1. Flow chart of methodology for delineation of clean-ice (CI) and debris-covered (DC) glaciers. Note. NDSI = Normalized Difference Snow Index. NDVI = Normalized Difference Vegetation Index.

Difference Snow Index (NDSI) (Hall, Riggs, & Salomonson, 1995; Racoviteanu, Williams, & Barry, 2008) was used to make an initial selection of segments for CI glaciers. In the next filtering step, different variables such as the Normalized Difference Vegetation Index (NDVI) (for vegetation), Land and Water Mask (for open water), mean slope and mean altitude were determined to identify misclassified image objects, which were excluded. The DC glaciers were captured from the segmented image objects using a slope threshold value of less than 25° , which captures the entire DC glacier area including vegetation, water, snow and surroundings. As DC glaciers only occur below 6000 masl, image objects outside the elevation range of 3000–6000 masl were excluded. Further threshold values of NDVI (>0.3), LWM (50–115.8) and NDSI (≥ 0.005) were used to exclude vegetation, snow, and land and water bodies, respectively. The filtering steps were not necessarily done in this order.

These processes satisfactorily delineated the outlines of CI and DC glaciers, which were then merged to a single file. Image objects with a surface area of less than 0.02 km^2 were then omitted and the edges of the polygons smoothed. The glacier image objects were transferred to a GIS-compatible format and finalized by manual editing at a scale of 1:20,000 by draping over respective images and verifying with high-resolution images from Google Earth in a GIS environment. Special attention was given to defining the outline and snout of the glaciers. CI glaciers require minor manual corrections; DC glaciers need careful manual corrections because they closely resemble moraines and bare rock outcrops.

For the time-series analysis, glacier polygons were generated for 2010 for the Wakhan, Shyok, Imja and Lunana areas using the method described above. The glacier outlines for the other decades were then generated by manual editing on the recent glacier outline, overlaying the Landsat images from 2000, 1990, and ~ 1980 .

Glacier attributes

Attribute data are assigned to each glacier polygon following international conventions set out by the World Glacier Monitoring Service, the GlobGlacier initiative, and the GLIMS community (Müller, Cafilisch, & Müller, 1977; Paul et al., 2010; Raup et al., 2007). For each glacier, a GLIMS ID, location, area, elevation range, aspect, average slope, mean glacier thickness, and estimated ice reserves were stored in the database. Further details of the method are given by Bajracharya and Shrestha (2011).

Uncertainty

The uncertainty of the glacier area depends on image resolution and snow cover. To minimize the uncertainty, images with the least snow cover were used, and the automatically derived glacier polygons were refined manually by draping over high-resolution Google Earth images. The maximum offset of the boundary cannot be greater than half of the image resolution (i.e. $\pm 15 \text{ m}$ for TM and ETM + and $\pm 30 \text{ m}$ for MSS). The steps to define the uncertainty of the glacier polygon were as follows:

- Buffering of mapped glacier polygons with half of the image pixels
- Calculation of the total number of pixels bounded by each buffered glacier polygon
- Calculation of buffered area by multiplying total pixel count and the area of one pixel
- Uncertainty of the mapped glacier taken as the variance in glacier area – that is, the difference between actual glacier area (mapped glacier polygon) and buffered glacier polygon area

The uncertainty of the glacier areas in the present study was 7% for ~1980 and 6% for 1990, 2000 and 2010.

Results

Glaciers in the HKH region

In total, 54,252 glaciers were identified within the HKH region, with a total area of 60,054 km² and estimated ice reserves of 6127 km³ (Figure 2, Table 1). This reveals that only 1.4% of the HKH region is glaciated; the total ice reserves are roughly equal to three times the annual precipitation (Bookhagen & Burbank, 2006; Immerzeel et al., 2010). There is a large variation between river basins; the largest total glacier areas are found in the Indus, Brahmaputra and Ganges basins, respectively (Figure 3).

Over 60% of the total glacier area of the HKH is located in the elevation range 5000–6000 masl (Figure 4). The glaciers below 5700 masl are particularly sensitive to climate change unless they are covered by thick debris (Bajracharya et al., 2014). The Indus, Ganges and Brahmaputra basins have 79%, 60% and 77% of their total glacier area, respectively, below this critical elevation. CI glaciers at low altitude and small glaciers are the most sensitive glaciers to climate change in the HKH region.

A thick debris layer has a strong insulating effect; sub-debris melt rates can be a factor of 5 to 10 lower than for CI glaciers (Hagg, Mayer, Lambrecht, & Helm, 2008; Mihalcea et al., 2006). A total of 32,000 km² of the glacier area was categorized as either DC or CI (glaciers within China were not differentiated). Of this, 9.7% overall was classified as DC, and 9.3%, 11.1% and 12.6% of the differentiated area in the Indus, Brahmaputra and Ganges basins, respectively. DC glaciers are mostly found at the frontal part of valley glaciers and have an average slope of 12° – much less steep than CI glaciers, which have an average slope of 25° (Bajracharya & Shrestha, 2011; Bolch et al., 2012).

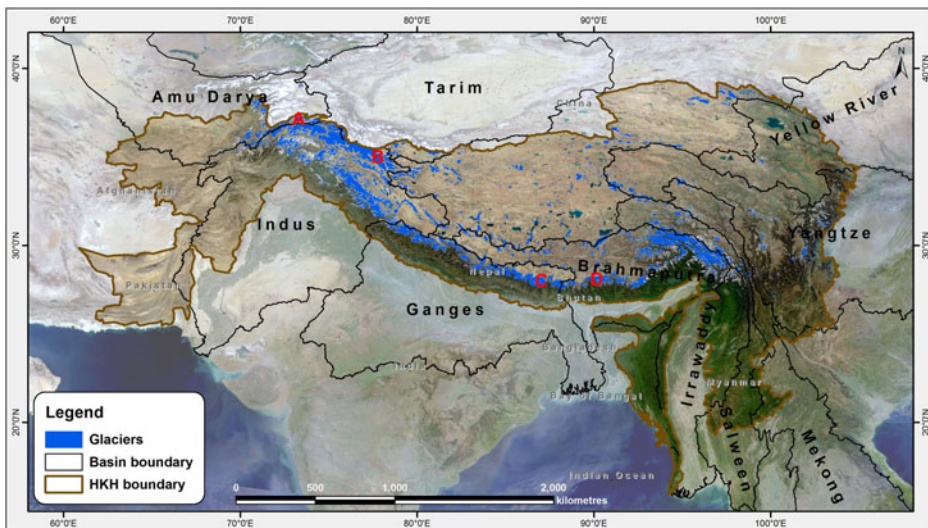


Figure 2. The Hindu Kush Himalayas (brown polygons), major river basins (black polygons) and glacier outlines (blue shaded polygons); red letters indicate the representative glaciers for which decadal changes are shown. *Note.* A = Wakhan Corridor, Afghanistan. B = Shyok Basin, Pakistan. C = Imja Valley, Nepal. D = Lunana area, Bhutan.

Table 1. Glacier characteristics in the basins of the Hindu Kush Himalayan region.

| Parameter | Basin | | | | | | | | | | | |
|------------------------|-----------|-----------|-----------|-------------|-----------|---------|---------|-----------|-----------|---------|----------|-----------|
| | Amu Darya | Indus | Ganges | Brahmaputra | Irrawaddy | Salween | Mekong | Yangtze | Yellow | Tarim | Interior | HKH |
| Basin area total | 645,726 | 1,116,086 | 1,001,019 | 528,079 | 426,501 | 363,778 | 841,322 | 2,065,763 | 1,073,168 | 929,003 | n/a | 8,991,813 |
| Basin area in the HKH | 166,686 | 555,450 | 244,806 | 432,480 | 202,745 | 211,122 | 138,876 | 565,102 | 250,540 | 26,729 | 909,824 | 3,705,721 |
| Latitude minimum | 34.57 | 30.45 | 27.53 | 27.49 | 28.06 | 28.38 | 28.3 | 28.20 | 33.29 | 34.74 | 29.69 | 27.49 |
| Latitude maximum | 38.35 | 37.08 | 31.42 | 31.03 | 28.77 | 32.76 | 33.73 | 35.77 | 38.25 | 36.74 | 39.28 | 39.28 |
| Longitude minimum | 67.63 | 69.36 | 77.98 | 82.03 | 98.17 | 91.5 | 94.15 | 90.55 | 98.61 | 75.56 | 78.31 | 67.63 |
| Longitude maximum | 74.88 | 81.65 | 88.7 | 97.76 | 97.86 | 98.71 | 98.76 | 103.89 | 101.87 | 86.81 | 100.54 | 103.89 |
| Number of glaciers | 3,277 | 18,495 | 7,963 | 11,497 | 133 | 2,113 | 482 | 1,661 | 189 | 1,091 | 7,351 | 54,252 |
| CI glacier area* | 2,406 | 15,635 | 5,622 | 1,186 | 35 | n/a | n/a | n/a | n/a | 517 | n/a | n/a |
| DC glacier area* | 161 | 1,970 | 810 | 148 | 0 | n/a | n/a | n/a | n/a | 32 | n/a | n/a |
| Total glacier area | 2,566 | 21,193 | 9,012 | 14,020 | 35 | 1,352 | 235 | 1,660 | 137 | 2,310 | 7,535 | 60,054 |
| Largest glacier area | 40 | 926 | 177 | 204 | 3 | 40 | 10 | 55 | 21 | 239 | 84 | 926 |
| Total ice reserves | 162.6 | 2,696.1 | 793.5 | 1,302.6 | 1.3 | 87.7 | 10.7 | 121.4 | 9.2 | 378.6 | 563.1 | 6,126.9 |
| Highest elevation | 7,213 | 8,566 | 8,806 | 8,331 | 4,256 | 6,471 | 6,361 | 6,270 | 5,710 | 6,462 | 6,609 | 8,806 |
| Lowest elevation | 3,131 | 2,409 | 3,273 | 2,435 | 5,695 | 3,786 | 2,891 | 2,972 | 4,151 | 3,940 | 3,994 | 2,409 |
| CI elevation minimum* | 3,415 | 2,723 | 3,610 | 3,707 | 4,256 | n/a | n/a | n/a | n/a | 4,277 | n/a | n/a |
| CI elevation maximum* | 7,213 | 8,566 | 8,806 | 8,331 | 5,695 | n/a | n/a | n/a | n/a | 6,462 | n/a | n/a |
| DC elevation minimum* | 3,131 | 2,409 | 3,273 | 3,882 | n/a | n/a | n/a | n/a | n/a | 3,940 | n/a | n/a |
| DC elevation maximum* | 5,466 | 5,913 | 6,009 | 5,828 | n/a | n/a | n/a | n/a | n/a | 5,235 | n/a | n/a |
| Mean CI glacier slope* | 25 | 25 | 28 | 25 | 25 | n/a | n/a | n/a | n/a | 17 | n/a | n/a |
| Mean DC glacier slope* | 12 | 11 | 12 | 13 | n/a | n/a | n/a | n/a | n/a | 10 | n/a | n/a |
| Mean slope | 24 | 24 | 28 | 25 | 25 | 25 | 26 | 27 | 26 | 26 | 24 | 25 |
| Average glacier area | 0.78 | 1.15 | 1.13 | 1.22 | 0.27 | 0.64 | 0.49 | 1.00 | 0.73 | 2.12 | 1.02 | 1.11 |

Note. Based on UTM, WGS 84 projection. HKH area = 4,192,446 km²; 10 basins' area in the HKH region = 2,795,898 km² (excluding the interior basin). Part of the HKH area is not included in either the 10 basins or the interior. n/a = not applicable (as not evaluated). CI = clean-ice. DC = debris-covered.

* Excluding glaciers in China.

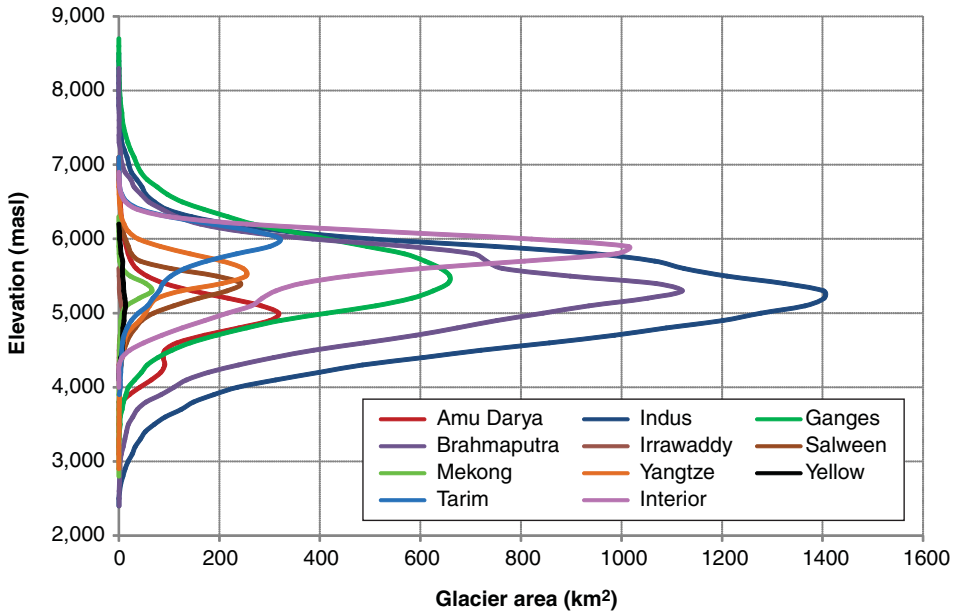


Figure 3. Glacier hypsographs of the major basins in the HKH region.

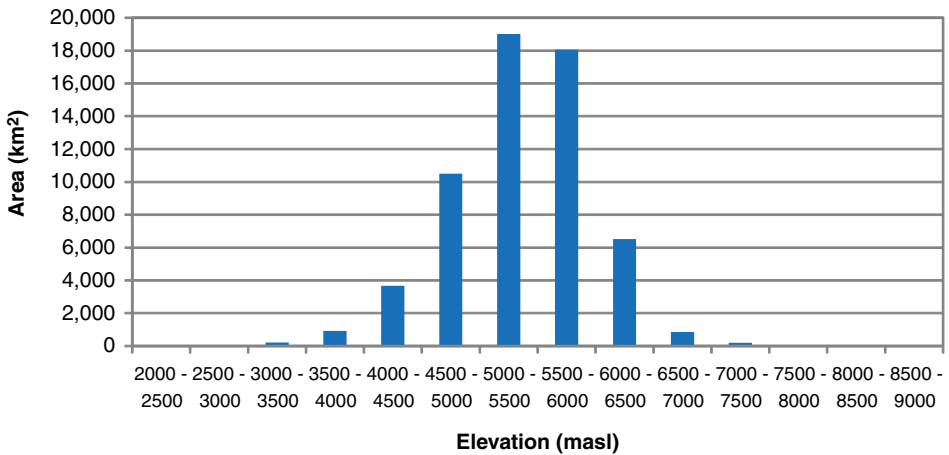


Figure 4. Glacier area distribution in 500 m elevation bands in the HKH region.

Glacier change in the selected basins

The time series analysis showed that the glacier area in the Wakhan Corridor is relatively stable (Figure 5, Table 2). Some glaciers showed small losses of area of less than 5% in the period 1980–1990; there were more noticeable area losses of 4–36% in 1990–2000, while most areas were stable or even increased in the period 2000–2010. Over the 30 years, most glaciers showed a slight reduction in glacier area, which was most prominent at the glacier tongues (Figure 5, panel A). Among the individual glaciers, no. 8 increased slightly in area over the 30 years; nos. 1 and 6 showed small losses of around 5% of area;

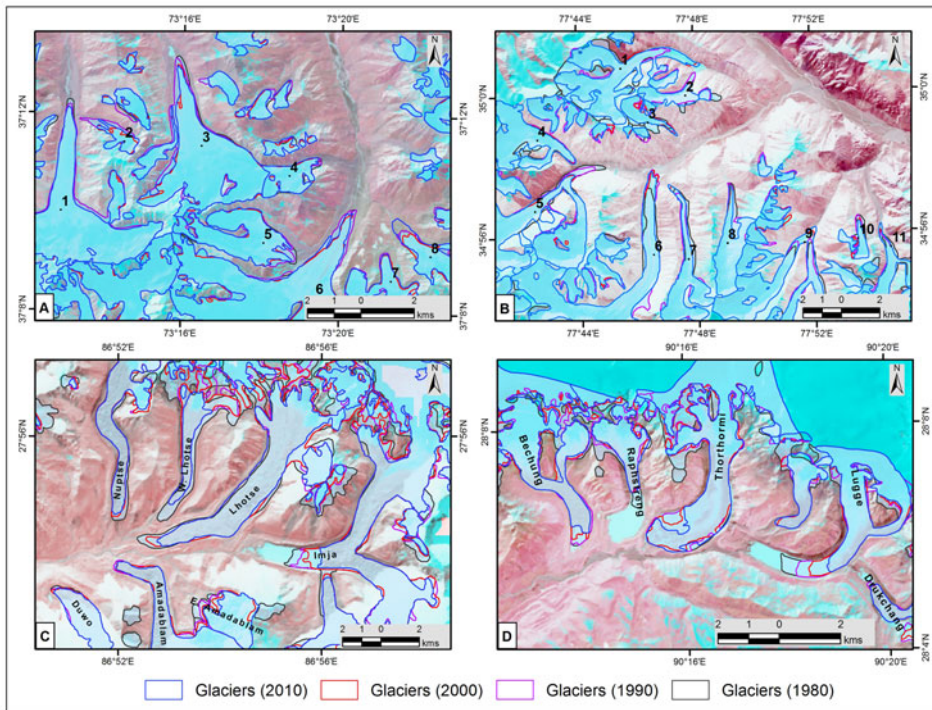


Figure 5. Representative examples of glacier change in different parts of the Hindu Kush Himalayan region. *Note.* A = Wakhan Corridor, Afghanistan. B = Shyok Basin, Pakistan. C = Imja Valley, Nepal. D = Lunana area, Bhutan.

the smallest glacier, no. 2, had a marked loss of 27% of area; and all other glaciers showed losses of 10–12% of area.

Most of the glaciers in the Shyok Basin lost area and retreated in the period 1980–1990, showed little change in 1990–2000, and remained static or advanced in 2000–2010. Over the 30 years, most glaciers showed some loss of area, but there was almost no change in the area of the largest glacier, no. 5.

The glaciers in the Imja Valley in Nepal and the Lunana region in Bhutan showed similar trends, with the highest losses of glacier area observed in the periods 1980–1990 and 2000–2010. The glaciers in the Himalaya are retreating faster than those in the Hindu Kush and Karakorum, with losses over 30 years of 5–55% of area. The West Lhotse Glacier in the Imja Valley was the fastest-retreating glacier of all those studied.

Discussion

The evaluation of glacier status using remote sensing provides baseline information on extension, aspect, slope, elevation, and type of glaciers. Complete inventories for different time series are needed to fully understand the likely future challenges for glacier meltwater resources and glacial hazards. The glaciers of the HKH region are situated above 3200 masl, and field-based mapping is difficult given the high altitude, remoteness, harsh climatic conditions and lack of logistical support. This limits our understanding of the spatial patterns of glacier dynamics and their sensitivity to climate variability across the Himalayas at a large scale. Until the launch of Landsat TM in 1982, compilation of glacier

Table 2. Representative examples of glacier change in the Hindu Kush Himalayan region.

| Basin | No. | GLIMS ID/Name | Glacier area (km ²) | | | | | Glacier area change (%) | | | | |
|--------------------|-----------------|----------------|---------------------------------|-------------|-------------|-------------|-----------|-------------------------|-----------|-----------|-------|--|
| | | | 1980 | 1990 | 2000 | 2010 | 1980-1990 | 1990-2000 | 2000-2010 | 1980-2010 | | |
| A. Wakhan Corridor | 1 | G073222E37165N | 11.1 ± 0.8 | 11 ± 0.4 | 10.5 ± 0.4 | 10.5 ± 0.4 | -0.9 | -4.5 | 0.0 | -5.4 | | |
| | 2 | G073242E37192N | 1.1 ± 0.23 | 1.1 ± 0.11 | 0.7 ± 0.09 | 0.8 ± 0.1 | 0.0 | -36.4 | 14.3 | -27.3 | | |
| | 3 | G073276E37183N | 11.9 ± 0.82 | 11.7 ± 0.41 | 10.4 ± 0.47 | 10.5 ± 0.47 | -1.7 | -11.1 | 1.0 | -11.8 | | |
| | 4 | G073311E37179N | 2 ± 0.22 | 1.9 ± 0.12 | 1.8 ± 0.12 | 1.8 ± 0.12 | -5.0 | -5.3 | 0.0 | -10.0 | | |
| | 5 | G073296E37157N | 5.5 ± 0.54 | 5.3 ± 0.27 | 5 ± 0.29 | 4.9 ± 0.3 | -3.6 | -5.7 | -2.0 | -10.9 | | |
| | 6 | G073306E37138N | 17.9 ± 1.31 | 17.9 ± 0.65 | 16.7 ± 0.67 | 17.1 ± 0.69 | 0.0 | -6.7 | 2.4 | -4.5 | | |
| | 7 | G073355E37143N | 4 ± 0.37 | 3.9 ± 0.18 | 3.6 ± 0.2 | 3.6 ± 0.21 | -2.5 | -7.7 | 0.0 | -10.0 | | |
| | 8 | G073375E37154N | 3 ± 0.4 | 3 ± 0.2 | 2.7 ± 0.2 | 3.1 ± 0.22 | 0.0 | -10.0 | 14.8 | 3.3 | | |
| | 1 | G077760E35012N | 12.4 ± 0.35 | 9.8 ± 0.6 | 10.5 ± 0.64 | 10.4 ± 0.66 | -21.0 | 7.1 | -1.0 | -16.1 | | |
| | 2 | G077783E34999N | 2.2 ± 0.07 | 2 ± 0.14 | 2 ± 0.13 | 2 ± 0.13 | -9.1 | 0.0 | 0.0 | -9.1 | | |
| B. Shyok Basin | 3 | G077770E34989N | 2.4 ± 0.1 | 1.9 ± 0.17 | 1.9 ± 0.17 | 2.1 ± 0.17 | -20.8 | 0.0 | 10.5 | -12.5 | | |
| | 4 | G077711E34982N | 8.1 ± 0.16 | 7.7 ± 0.36 | 7.8 ± 0.35 | 7.6 ± 0.37 | -4.9 | 1.3 | -2.6 | -6.2 | | |
| | 5 | G077724E34958N | 29.3 ± 0.88 | 30 ± 1.16 | 29.4 ± 1.11 | 29.5 ± 1.13 | 2.4 | -2.0 | 0.3 | 0.7 | | |
| | 6 | G077774E34919N | 17.1 ± 0.48 | 17.2 ± 0.69 | 16.5 ± 0.69 | 16.6 ± 0.69 | 0.6 | -4.1 | 0.6 | -2.9 | | |
| | 7 | G077792E34912N | 6.7 ± 0.05 | 6.2 ± 0.37 | 6 ± 0.35 | 6 ± 0.35 | -7.5 | -3.2 | 0.0 | -10.4 | | |
| | 8 | G077815E34923N | 5.5 ± 0.19 | 5 ± 0.25 | 4.9 ± 0.25 | 5 ± 0.25 | -9.1 | -2.0 | 2.0 | -9.1 | | |
| | 9 | G077865E34917N | 21.2 ± 0.52 | 20.3 ± 1.05 | 20.5 ± 1.06 | 20.6 ± 1.06 | -4.2 | 1.0 | 0.5 | -2.8 | | |
| | 10 | G077894E34926N | 1.7 ± 0.03 | 1.5 ± 0.13 | 1.3 ± 0.15 | 1.2 ± 0.13 | -11.8 | -13.3 | -7.7 | -29.4 | | |
| | 11 | G077910E34918N | 8.5 ± 0 | 7.6 ± 0.52 | 7.5 ± 0.52 | 7.6 ± 0.53 | -10.6 | -1.3 | 1.3 | -10.6 | | |
| | C. Imjia Valley | 1 | Nuptse | 5.5 ± 0.64 | 4.2 ± 0.31 | 4.3 ± 0.3 | 4 ± 0.29 | -23.6 | 2.4 | -7.0 | -27.3 | |
| 2 | | West Lhotse | 5.1 ± 0.57 | 3.4 ± 0.31 | 3.4 ± 0.3 | 2.3 ± 0.27 | -33.3 | 0.0 | -32.4 | -54.9 | | |
| 3 | | Lhotse | 14.7 ± 1.32 | 13.1 ± 0.72 | 12.1 ± 0.7 | 10.2 ± 0.68 | -10.9 | -7.6 | -15.7 | -30.6 | | |
| 4 | | Imjia | 21 ± 1.67 | 20.1 ± 0.96 | 19.4 ± 0.89 | 17.6 ± 0.9 | -4.3 | -3.5 | -9.3 | -16.2 | | |
| 5 | | East Amadablam | 2.3 ± 0.13 | 2.2 ± 0.08 | 2 ± 0.08 | 1.9 ± 0.08 | -4.3 | -9.1 | -5.0 | -17.4 | | |
| 6 | | Amadablam | 6.9 ± 0.68 | 6.5 ± 0.31 | 6.2 ± 0.3 | 6 ± 0.3 | -5.8 | -4.6 | -3.2 | -13.0 | | |
| D. Lunana area | 7 | Duwo | 1.9 ± 0.23 | 1.8 ± 0.11 | 1.9 ± 0.1 | 1.8 ± 0.1 | -5.3 | 5.6 | -5.3 | -5.3 | | |
| | 1 | Bechung | 10.2 ± 0.82 | 9.2 ± 0.59 | 9 ± 0.56 | 8.3 ± 0.54 | -9.8 | -2.2 | -7.8 | -18.6 | | |
| | 2 | Raphstreng | 4.1 ± 0.46 | 3.1 ± 0.27 | 3 ± 0.27 | 2.9 ± 0.24 | -24.4 | -3.2 | -3.3 | -29.3 | | |
| | 3 | Thorthormi | 15.2 ± 0.92 | 13.5 ± 0.62 | 13.4 ± 0.61 | 13 ± 0.62 | -11.2 | -0.7 | -3.0 | -14.5 | | |
| | 4 | Lugge | 6.6 ± 0.63 | 6.1 ± 0.34 | 5.6 ± 0.32 | 5.2 ± 0.29 | -7.6 | -8.2 | -7.1 | -21.2 | | |
| 5 | Drukchang | 7.3 ± 0.49 | 7.5 ± 0.28 | 7.1 ± 0.27 | 6.7 ± 0.23 | 2.7 | -5.3 | -5.6 | -8.2 | | | |

inventories was challenging and mostly based on existing topographic maps. Over the past several years, remote sensing–based inventories for several parts of the HKH region have been entered into the GLIMS database (Raup et al., 2007). However, different methods and data sources have been used (topographic maps based on aerial photos with limited field inputs, satellite images), with acquisition dates that are years to decades apart. This underlines the need for a homogeneous method from a single source of data using recent imagery acquired within a short time span.

The changes in glaciers can be assessed from time series of images. The selected basins cover a representative range of climates and glacier systems (Figure 2). A time series analysis was performed using a homogeneous source of images (Figure 5, Table 2) to assess the glacier change.

A slight reduction in glacier extent was observed consistently in all glacier tongues in the Wakhan Corridor (Figure 5, panel A). The glaciers in the Shyok Basin in the Karakorum showed a different pattern, with glaciers advancing and tributaries merging, especially during the last decade, consistent with earlier reports (Archer & Fowler, 2004; Hewitt, 2005, 2011; Scherler et al., 2011; Tahir et al., 2011). Glaciers in the Himalayas (Figure 5, panels C and D) showed consistent retreat in both Nepal and Bhutan. Some ice-apron glaciers have disappeared from the mountain slopes, and glaciers are increasingly fragmented. These glaciers are all characterized by synchronous ablation and accumulation during the monsoon season and are particularly sensitive to climate perturbations (Immerzeel, Van Beek, Konz, Shrestha, & Bierkens, 2012). The Imja Lake in Nepal (Figure 5, panel C) is one of the fastest-growing lakes in the Himalayas, and the DC glacier that connects to the lake has retreated much faster than other nearby DC glaciers (Bajracharya et al., 2007). The same phenomenon was observed in the DC glaciers that connect to the Raphstreng, Thorthormi and Luggye glacial lakes in the Lunana region in Bhutan (Figure 5, panel D).

The distribution of individual glaciers is important, as small glaciers (Glacier 2 in the Wakhan Corridor, Glacier 10 in the Shyok Basin, West Lhotse Glacier in the Imja Valley, and Raphstreng Glacier in the Lunana area) are more sensitive to climate change than large glaciers (Bahr, Meier, & Peckham, 1997). A large proportion of the total ice area in the Ganges and Brahmaputra Basins is contributed by small glaciers. The distribution of the total ice area over different elevation bands is another crucial determinant for climate change sensitivity.

We suggest that in the Hindu Kush glaciers are retreating slowly but steadily, while in the Karakoram glaciers show a mixed response, varying from thinning of large DC tongues to advancing and surging tributaries. In the Himalayas, glaciers are retreating rapidly, with a marked catalytic role played by glacial lakes. However, a complete regional understanding will require multi-temporal comprehensive glacier inventories in combination with high-resolution climate datasets.

Conclusions

A large step has been taken in compiling a reference cryospheric dataset for the entire HKH region which is publicly available and can be used as a benchmark against which changes can be assessed. The challenge now is to maintain this dataset and to further extend it by increasing the temporal interval as far back into the past as available imagery allows.

Larger glaciers (exceeding 15 km² in Shyok and the Wakhan Corridor have shown no significant change in area; however, the smaller glaciers are retreating faster. The glaciers

in the Wakhan Corridor retreated faster in 1990–2000; the glaciers in the other regions retreated faster in 1980–1990. The retreat rate was slower in 2000–2010 in all basins, and some glaciers in the Wakhan Corridor and Shyok Basin showed some advance.

The cryosphere in the HKH region is changing; however, the downstream impact remains uncertain. We formulate four key challenges that need to be addressed before we can arrive at detailed spatially explicit projections of water availability. (1) Precipitation drives the accumulation of glaciers, but spatio-temporal quantifications of the present climate, let alone future projections, are highly uncertain. (2) There are no fully distributed hydrological models available at the regional scale that include the cryosphere with a sufficient level of detail to assess future change in water availability. (3) Glacial melt and snowmelt are complex energy-balance processes which are influenced by debris cover, black carbon deposition, albedo feedback, and sublimation; these processes are poorly understood, and the data needed to derive a full energy balance and resulting melt rates is generally lacking at high altitude. (4) There is a need for robust algorithms that quantify future glacier extent as a function of model forcing and surface features.

Acknowledgements

The authors thank the Cryosphere Monitoring Project of the Swedish International Development Cooperation Agency and the Norwegian Ministry of Foreign Affairs for their support to undertake the mapping and monitoring of glaciers in the HKH region. Partial support was provided by the HIMALA and Servir Himalaya projects of OFDA, NASA and USAID. The Landsat images were downloaded from USGS.

Disclosure statement

No potential conflict of interest was reported by the authors.

References

- Archer, D. R., & Fowler, H. J. (2004). Spatial and temporal variations in precipitation in the Upper Indus Basin, global teleconnections and hydrological implications. *Hydrology and Earth System Sciences*, 8, 47–61. doi:10.5194/hess-8-47-2004
- Bahr, D., Meier, M., & Peckham, S. (1997). The physical basis of glacier volume-area scaling. *Journal of Geophysical Research*, 102, 20355–20362. doi:10.1029/97JB01696
- Bajracharya, S. R., Maharjan, S. B., & Shrestha, F. (2014). The status and decadal change of glaciers in Bhutan from 1980s to 2010 based on the satellite data. *Annals of Glaciology*, 55, 159–166. doi:10.3189/2014AoG66A125
- Bajracharya, S. R., & Mool, P. K. (2010). Glaciers, glacial lakes and glacial lake outburst floods in the Mount Everest region, Nepal. *Annals of Glaciology*, 50, 81–86. doi:10.3189/172756410790595895
- Bajracharya, S. R., Mool, P. K., & Shrestha, B. R. (2007). *Impact of climate change on Himalayan glaciers and glacial lakes: Case studies on GLOF and associated hazards in Nepal and Bhutan*. Kathmandu: ICIMOD.
- Bajracharya, S. R., & Shrestha, B. (Eds.). (2011). *The status of glaciers in the Hindu Kush-Himalayan region*. Kathmandu: ICIMOD.
- Bolch, T., Kulkarni, A., Kääb, A., Huggel, C., Paul, F., Cogley, J. G., & ... Stoffel, M. (2012). The state and fate of Himalayan glaciers. *Science*, 336, 310–314. doi:10.1126/science.1215828
- Bookhagen, B., & Burbank, D. W. (2006). Topography, relief, and TRMM-derived rainfall variations along the Himalaya. *Geophysical Research Letters*, 33(8), 1–5. doi:10.1029/2006GL026037
- Dyhrenfurth, G. O. (1955). *The third Pole – The history of the High Himalaya* (1st UK Edition). London: Ex Libris, Werner Laurie.

- Fujita, K., & Nuimura, T. (2011). Spatially heterogeneous wastage of Himalayan glaciers. *Proceedings of the National Academy of Sciences*, *108*, 14011–14014. doi:10.1073/pnas.1106242108
- Haerberli, W., Böschi, H., Sherler, K., Østrem, G., & Wallèn, C. C. (Eds.). (1989). *World glacier inventory Status 1988*. Wallingford: IAHS.
- Hagg, W., Mayer, C., Lambrecht, A., & Helm, A. (2008). Sub-debris melt rates on southern Inylchek Glacier, Central Tian Shan. *Geografiska Annaler, Series A: Physical Geography*, *90*, 55–63. doi:10.1111/j.1468-0459.2008.00333.x
- Hall, D. K., Riggs, G. A., & Salomonson, V. V. (1995). Development of methods for mapping global snow cover using moderate resolution imaging spectroradiometer data. *Remote Sensing of Environment*, *52*, 127–140.
- Hewitt, K. (2005). The Karakoram anomaly? Glacier expansion and the “elevation effect.” Karakoram Himalaya. *Mountain Research and Development*, *25*, 332–340. doi:10.1659/0276-4741(2005)025[0332:TKAGEA]2.0.CO;2
- Hewitt, K. (2011). Glacier change, concentration, and elevation effects in the Karakoram Himalaya, Upper Indus Basin. *Mountain Research and Development*, *31*, 188–200. doi:10.1659/MRD-JOURNAL-D-11-00020.1
- Immerzeel, W. W., Van Beek, L. P. H., & Bierkens, M. F. P. (2010). Climate change will affect the Asian water towers. *Science*, *328*, 1382–1385. doi:10.1126/science.1183188
- Immerzeel, W. W., Van Beek, L. P. H., Konz, M., Shrestha, A. B., & Bierkens, M. F. P. (2012). Hydrological response to climate change in a glacierized catchment in the Himalayas. *Climatic Change*, *110*, 721–736. doi:10.1007/s10584-011-0143-4
- Kargel, J. S., Cogley, J. G., Leonard, G. J., Haritashya, U., & Byers, A. (2011). Himalayan glaciers: The big picture is a montage. *Proceedings of the National Academy of Sciences*, *108*, 14709–14710. doi:10.1073/pnas.1111663108
- Kaser, G., Cogley, J. G., Dyurgerov, M. B., Meier, M. F., & Ohmura, A. (2006). Mass balance of glaciers and ice caps: Consensus estimates for 1961–2004. *Geophysical Research Letters*, *33*(19), 1–5. doi:10.1029/2006GL027511
- Kaser, G., Großhauser, M., & Marzeion, B. (2010). Contribution potential of glaciers to water availability in different climate regimes. *Proceedings of the National Academy of Sciences of the United States of America*, *107*, 20223–20227. doi:10.1073/pnas.1008162107
- Mihalcea, C., Mayer, C., Diolaiuti, G., Lambrecht, A., Smiraglia, C., & Tartari, G. (2006). Ice ablation and meteorological conditions on the debris-covered area of Baltoro glacier, Karakoram, Pakistan. *Annals of Glaciology*, *43*, 292–300. doi:10.3189/172756406781812104
- Müller, F., Caffisch, T., & Müller, G. M. (1977). *Instructions for the compilation and assemblage of data for a world glacier inventory*. Zurich: Department of Geography, Swiss Federal Institute of Technology (ETH).
- Paul, F., Barry, R. G., Cogley, J. G., Frey, H., Haerberli, W., Ohmura, A., & ... Zemp, M. (2010). Recommendations for the compilation of glacier inventory data from digital sources. *Annals of Glaciology*, *50*, 119–126. doi:10.3189/172756410790595778
- Pfeffer, W. T., Arendt, A. A., Bliss, A., Bolch, T., Cogley, J. G., Gardner, A. S., ... Sharp, M. J. & the Randolph Consortium. (2014). The Randolph Glacier Inventory: a globally complete inventory of glaciers. *Journal of Glaciology*, *60*, 537–552. doi:10.3189/2014JG13J176
- Rabatel, A., Francou, B., Soruco, A., Gomez, J., Cáceres, B., Ceballos, J. L., & ... Wagnon, P. (2013). Current state of glaciers in the tropical Andes: A multi-century perspective on glacier evolution and climate change. *The Cryosphere*, *7*, 81–102. doi:10.5194/tc-7-81-2013
- Racoviteanu, A. E., Williams, M. W., & Barry, R. G. (2008). Optical remote sensing of glacier characteristics: A review with focus on the Himalaya. *Sensors*, *8*, 3355–3383. doi:10.3390/s8053355
- Rankl, M., Kienholz, C., & Braun, M. (2014). Glacier changes in the Karakoram region mapped by multitemporal satellite imagery. *The Cryosphere*, *8*, 977–989. doi:10.5194/tc-8-977-2014
- Raup, B., Kaab, A., Kargel, J., Bishop, M., Hamilton, G., Lee, E., & ... Khalsa, S. (2007). Remote sensing and GIS technology in the Global Land Ice Measurements from Space (GLIMS) project. *Computers & Geosciences*, *33*, 104–125. doi:10.1016/j.cageo.2006.05.015
- Richardson, S. D., & Reynolds, J. M. (2000). An overview of glacial hazards in the Himalayas. *Quaternary International*, *65–66*, 31–47. doi:10.1016/S1040-6182(99)00035-X

- Scherler, D., Bookhagen, B., & Strecker, M. R. (2011). Spatially variable response of Himalayan glaciers to climate change affected by debris cover. *Nature Geoscience*, 4(1), 1–1. doi:[10.1038/ngeo1059](https://doi.org/10.1038/ngeo1059)
- Tahir, A. A., Chevallier, P., Arnaud, Y., & Ahmad, B. (2011). Snow cover dynamics and hydrological regime of the Hunza River basin, Karakoram Range, Northern Pakistan. *Hydrology and Earth System Sciences*, 15, 2275–2290. doi:[10.5194/hess-15-2275-2011](https://doi.org/10.5194/hess-15-2275-2011)
- Zemp, M., Hoelzle, M., & Haeberli, W. (2009). Six decades of glacier mass-balance observations: A review of the worldwide monitoring network. *Annals of Glaciology*, 50, 101–111. doi:[10.3189/172756409787769591](https://doi.org/10.3189/172756409787769591)